# Chapter 24

# Carbon Capture and Storage (CCS)

Helge Hellevang

## 24.1 Introduction

Carbon Capture and Storage (CCS) involves capturing $CO_2$ and then storing it so that it is not emitted to the atmosphere. The background for CCS is a concern that increasing atmospheric $CO_2$ concentrations will cause global climate changes, ocean acidification and a sea level rise, with dramatic negative consequences for large populations (IPCC 2013).

Although capture technologies in principle can be implemented for any natural gas or flue gas sources, costs put practical constrains on what kind of operations that can implement CCS. Generally, any large point source of $CO_2$ (>1 Mt $CO_2$/year), such as coal- or gas-fired power plants, natural gas producers and cement factories, has sufficient $CO_2$ production to justify installation of CCS technology. The cost may however be rather prohibitive.

$CO_2$ may be captured from major point sources. If several point sources are in the same geographical region, then captured $CO_2$ should be transported to a common hub before being injected into a geological formation (Fig. 24.1). This lowers the cost of implementing the pipeline network and thereby the total cost of the CCS operation. The geological storage units can be of various kinds, such as saline aquifers, coal seams and abandoned oil and gas fields. The requirement is that $CO_2$ is stored as a dense supercritical phase ($scCO_2$), that typically requires more than 700–800 m burial depth, and that the reservoir has a seal (cap rock), and sufficient injectivity (porosity and permeability) to store large volumes of $CO_2$. These issues are discussed below.

H. Hellevang (✉)
Department of Geosciences, University of Oslo, Oslo, Norway
e-mail: helge.hellevang@geo.uio.no

## 24.2 $CO_2$ Capture

Capture refers to the separation of $CO_2$ from natural gas or flue (exhaust) gas where the concentration of $CO_2$ may be as low as 3–4%. In CCS, capture is followed by transport and finally underground storage. There is considerable research activity to improve the efficiency of present-day capture methods and to invent new and better technologies, the main motivation being to reduce the cost of the capture process. Capture, whether it is by pre- or post-combustion, requires significant amounts of energy. For a coal-fired power plant, an extra 20–25% of energy is typically required for capturing and compressing the $CO_2$.

There are already several technologies available for capturing $CO_2$. A review of the advances in these technologies is provided by Figueroa et al. (2008) and only a brief overview will be given here. In post-combustion capture, $CO_2$ is removed from flue gases formed from the combustion of primarily coal. The coal is burned in an air atmosphere, in contrast to oxy-combustion that utilizes an oxygen atmosphere with little nitrogen. In pre-combustion capture, $CO_2$ is removed from the fuel before combustion. This technology is applied to gasification plants. In separating $CO_2$ from the gas streams, various technologies are being used, such as gas-phase separation, sorption to liquids or solids, and hybrid processes such as sorption/membrane systems. Each of these technologies has their strengths and weaknesses, and the choice of

K. Bjørlykke (ed.), *Petroleum Geoscience: From Sedimentary Environments to Rock Physics*,
DOI 10.1007/978-3-642-34132-8_24, © Springer-Verlag Berlin Heidelberg 2015

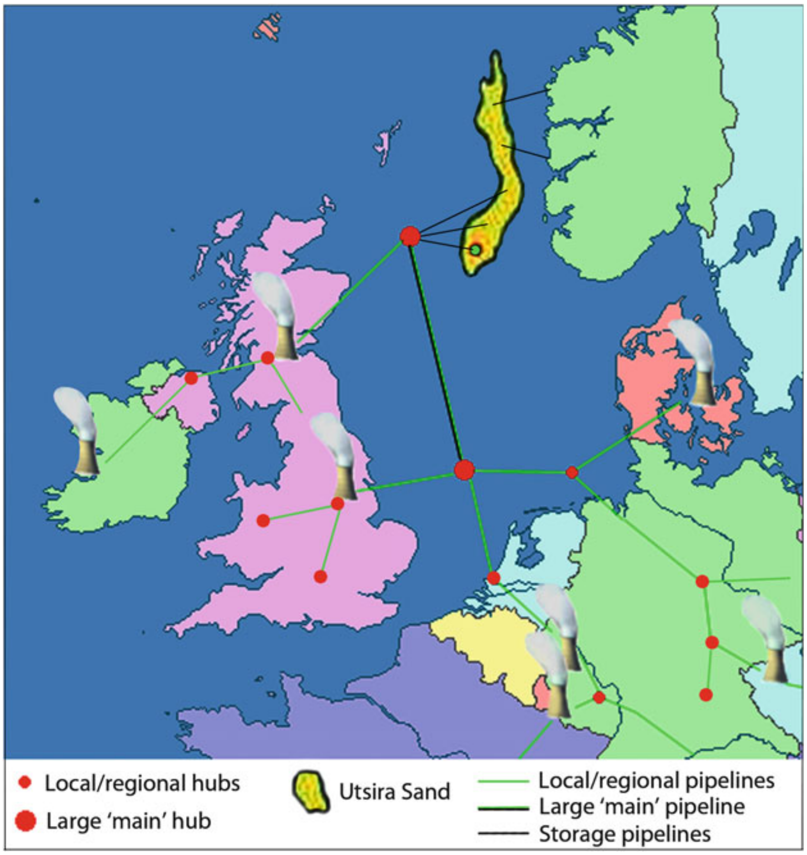


**Fig. 24.1** $CO_2$ can be captured at major point emitters, such as coal-fired power plants, and piped through a network of pipelines to major storage units, such as the Utsira Sand

technology must be based on the processing plant, and whether the technology will be implemented on existing plants (retrofit), or integrated into new plants.

## 24.3 What Is Required to Store $CO_2$?

### *24.3.1 $CO_2$ Point Sources*

Size matters in CCS. A large part of the cost of CCS is related to the capture facilities and the transport network to the $CO_2$ storage site (steel pipelines and compressors). The possibility of capturing large amounts of $CO_2$ at one plant lowers the cost of CCS (\$/ton stored $CO_2$). This is critical in order to implement CCS globally at a scale required to meet the IPCC 2°C target. CCS therefore requires point sources of $CO_2$, which can be cement factories, coal-fired power plants, or production facilities for natural gas (all with a potential of about 1–3 Mt $CO_2$/year). If several minor $CO_2$ point sources (<1 Mt/year) are in a geographically limited area, the sources (flue gas or natural gas) can be piped to a common capture facility. In addition to the size of the facilities, geographical location plays a role. Because of the costs and risks associated with pipelines, the distance to the storage reservoir should be as short as possible.

### *24.3.2 The Storage Reservoir: Injectivity and $CO_2$ Storage Capacity*

The requirements of a $CO_2$ storage deposit are to a large extent the same as those for petroleum reservoirs. Injection requires that the pressure of the injection well is larger than the reservoir pressure. The amount of overpressure required is given by the injectivity of the reservoir, which is determined by several factors, such as the size of the reservoir unit and its hydraulic conductivity. The size of the reservoir unit refers to the volume that can absorb the pressure build-up resulting from the $CO_2$ injection and formation water mobilisation. For extensive reservoir units such as the Utsira Sand, pressure is dispersed through a large volume and pressure build-up is minimal, and the injectivity is therefore very high. The Tubåen Formation at Snøhvit, on the other hand, is divided into pressure compartments by steep faults with low permeability and hydraulic conductivity, resulting in rapid pressure build-up (Pham et al. 2011). Hydraulic conductivity depends on the permeability of the reservoir and the viscosity of the fluid, with high permeabilities (and low viscosities) favouring water mobilisation and preventing pressure build-up.

A storage deposit must in addition to injectivity have sufficient capacity. If pressure build-up is not considered, $CO_2$ storage capacity for saline aquifers can be estimated by the following relationship (see $CO_2$ Storage Atlas Norwegian Sea, 2012):

$$m_{CO_2} = V_b \cdot \phi \cdot N/G \cdot \rho_{CO_2} \cdot \chi \tag{24.1}$$

where $V_b$, $\phi$, and $N/G$ are the bulk volume, porosity and Net/Gross ratio of the storage reservoir, $\rho_{CO_2}$ is the density of $CO_2$, and $\chi$ is the storage efficiency factor. We see that injectivity and storage capacity are linked through the reservoir volume and porosity (affecting permeability; see Chap. 10). The density of $CO_2$ varies from about 2 kg/m$^3$ at the Earth's surface (a bit heavier than air) to more than 500 kg/m$^3$ at conditions deep underground where $CO_2$ is supercritical. The $CO_2$ properties are described in more detail in section 24.4. From equation (24.1), we see that the storage capacity is proportional to the $CO_2$ density. The final variable is the storage efficiency factor. This is defined as the fraction of the total reservoir pore space that can be filled with $scCO_2$, with values typically being a few percent or lower. The most important factor controlling the storage efficiency factor is reservoir heterogeneity. Spatial differences in permeability lead to flow of $CO_2$ along preferential fluid pathways, and $CO_2$ is prevented by the capillary entry pressure from migrating into fine-grained units.

### *24.3.3 The Seal (Cap Rock)*

As for oil and natural gas, the density of $CO_2$ stored underground is lower than formation water, so $CO_2$ will migrate buoyantly towards the surface. The requirement of a seal or cap-rock is therefore analogous to petroleum reservoirs. Chapter 1 gives an overview over different structural and stratigraphic traps, and Chap. 12 explains the detailed tectonic and structural settings of hydrocarbon traps.

Although $CO_2$ storage is in many ways analogous to hydrocarbon storage, there is one important difference: $CO_2$ is reactive and forms carbonic acid that may react with, and change the properties of, the cap-rock (Alemu et al. 2011). The effect of this alteration on an intact caprock at ambient temperatures (for most cases probably at less than 100°C) is however likely very limited as the reactions are slow and diffusion of $CO_2$ into a tight shale will be very slow as well (Gaus et al. 2005; Lu et al. 2009). If $CO_2$ is allowed to migrate into fractures or faults that penetrate the seal, then the picture is more uncertain, and it is not well understood if and when reactions will be self-sealing, and when reactions will enhance flow.

## 24.4 The Fluid Properties of $CO_2$

$CO_2$ may occur as a solid, a liquid or a vapour, determined by the temperature and pressure (Fig. 24.2). Properties such as density and viscosity vary greatly between these phases. At 304.25 K and 7.38 MPa, $CO_2$ is at the so-called critical point (Crp), and above this point $CO_2$ is termed supercritical. At temperatures above the Crp (but pressure below), $CO_2$ is a critical gas, whereas if only pressure is above the Crp, $CO_2$ will be a critical liquid with high density similar to natural gas. The viscosity of $scCO_2$ is about 0.05–0.06 cp at 100 bar and 37°C (Zabaloy et al. 2005) (corresponding to the Utsira storage reservoir), slightly lower than for water under the same conditions. The storage capacity is a function of $CO_2$ density and therefore also of burial depth. At the Earth's surface, $CO_2$ takes up approximately 22.4 l/mol gas (about 0.51 l/g). At these conditions, only a couple of grams of $CO_2$ could have been stored per litre pore space. The situation is however very different at the higher temperatures and pressures found underground. The density of $CO_2$ increases with pressure and decreases with temperature in a quite complex way (Fig. 24.3). At low temperatures, below the Crp, pressure increases leads to a phase transition from gas to liquid and a large increase in the $CO_2$ density. Above the Crp, no such phase transitions occur and

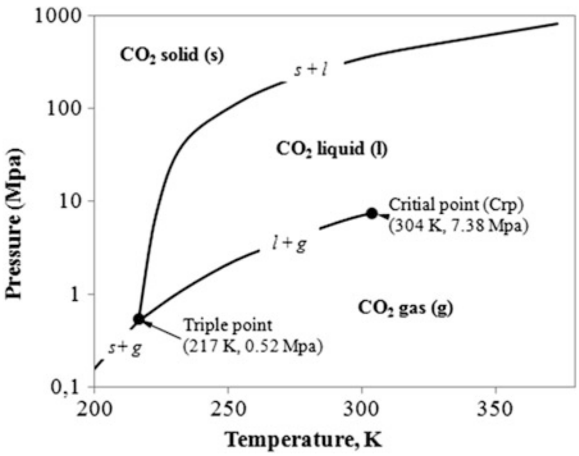


**Fig. 24.2** $CO_2$ phase stability diagram ($s$ = solid, $l$ = liquid, $g$ = gas). Phase boundaries are given by the *solid curves*, whereas the triple point ($T$ and $P$ where $s + l + g$ are all stable) and critical point (Crp) are indicated by *solid circles*

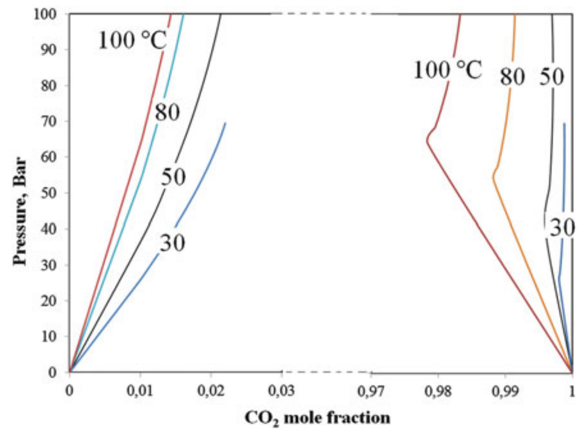


**Fig. 24.4** Mutual solubilities of $CO_2$ and $H_2O$. (**a**) The amount of $CO_2$ dissolved in the water-rich phase increases with pressure but decreases with temperature; (**b**) the amount of $H_2O$ dissolved in the $CO_2$-rich phase increases with temperature, whereas pressure first has a positive effect before the solubility decreases at increasing pressures. Calculations done by R. Miri (UiO) using the SAFT-EOS approach

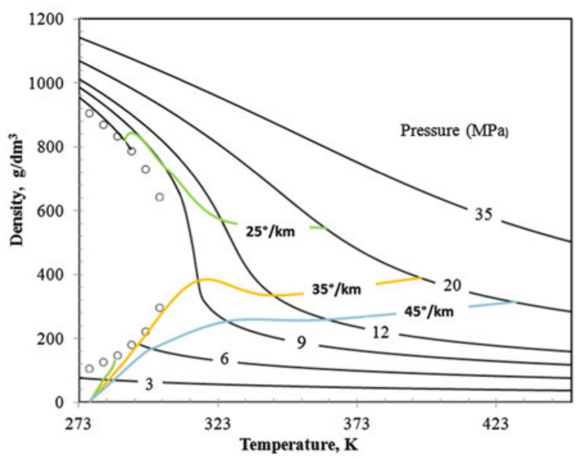


**Fig. 24.3** $CO_2$ densities as a function of temperature and pressure (from 0 to 70 Mpa and 273 to 453 K). Superimposed are $CO_2$ density curves estimated by three different geothermal gradients; one being a 'normal' North Sea gradient (35°/km) and two other curves being ±10°/km from the normal gradient. Density data from the NIST database

pressure increases lead to a steady increase in density. If $CO_2$ is stored underground at normal pressure (hydrostatic; see Chap. 10), the geothermal gradient determines the phase properties. Superimposed on the density plot in Fig. 24.3 are three geothermal gradients, one being quite average for the North Sea (35°C/km) and the two others being ±10°C/km. We see that there are large differences in density, especially at shallow depth. It is also clear that $CO_2$ storage reservoirs, which most likely will lie at depths greater than 1 km, $CO_2$ will have densities between about 200 and 700 g/cm$^3$ compared to >1,000 g/cm$^3$ for brine, giving a significant buoyancy, i.e. upward force.

To avoid corrosion of pipelines and formation of hydrates (ice-like particles of water and $CO_2$), $CO_2$ should be injected as a dry phase with as little water as possible in the stream. However, as soon as $CO_2$ is injected into a reservoir, $CO_2$ mixes and dissolves in water and some water dissolves back into the $CO_2$ phase and reacts to form carbonic acid. The mutual solubilities of $CO_2$ and water depend on temperature and pressure and on the salinity of the formation water. Although the mutual solubilities are quite limited (Fig. 24.4), they have profound effects on the storage operation both during the injection period (typically lasting for a few decades) and during the subsequent long-term storage.

During injection, water that is close to the well will dissolve into the dry $CO_2$ and the salinity of the brine will increase. This may result in the formation of evaporites, clogging the pore space and reducing the injectivity. The potential that one pore volume of brine has to change the porosity depends on the initial salinity. If the salinity is 1 mol NaCl/L pore space, a complete dry-out would clog approximately 3% of the pore space (assuming a halite molar weight and density of 58.44 g/mol and 2.17 g/cm$^3$ respectively).

This appears to be quite limited. However, as pores dry out, additional brine may be brought in by capillary suction and osmotic pressure differences, leading to further salt precipitation. Dissolution of $CO_2$ into water affects the storage operation on both short and long time-scales. First, dissolved $CO_2$ reacts with water and forms carbonic acid, and the pH may drop to 3 or even lower depending on the buffer capacity and $CO_2$ pressure. This results in dissolution of the minerals present in the reservoir and formation of new secondary phases. In hundreds to thousands of years, these mineral reactions may form carbonates, immobilising $CO_2$ for long time spans (see next section).

A second effect of dissolved $CO_2$ is that it increases the density of the water. The solubility of $CO_2$ at 100 bars and 37°C in a solution of normal seawater salinity (~0.5 mol NaCl per kg water (kgw)) is approximately 1.1 mol/kgw. At full $CO_2$ saturation, density is about 1,034 kg/m$^3$, which is 1.6% higher than the solution without $CO_2$ (about 1,018 kg/m$^3$). It has been suggested that the density contrast between $CO_2$-saturated formation water and normal brine may result in convection cells, making the heavier $CO_2$-charged solutions sink downwards, and bringing 'fresh' brine upwards which increases the dissolution rate of the sc$CO_2$ (Elenius and Gasda 2013). Viewed in the light of earlier studies on the possibility of density currents in stratified and vertically heterogeneous sandstones (Bjørlykke et al. 1988), conclusions on the extent of such mixing still have to be taken with caution. Moreover, the solubility of $CO_2$ in water is strongly a function of salt content. Higher salinities results in less dissolved $CO_2$ (Fig. 24.5), and less density contrast between fully saturated $CO_2$-brine and brine with no $CO_2$ (Fig. 24.6). The potential for density currents for high-salinity brines may therefore be even lower.

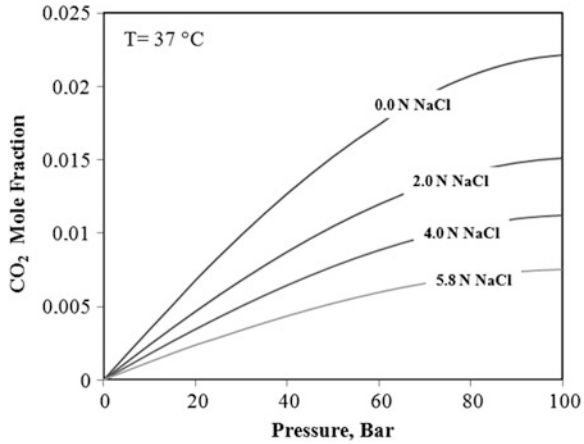


**Fig. 24.5** Solubility of $CO_2$ in NaCl-dominated brines with salt contents from 0.0 to 5.8 moles per kg water (kgw). Note the "salting out effect", how the solubility decreases with increasing salt content. Calculations done by R. Miri using the SAFT-EOS approach

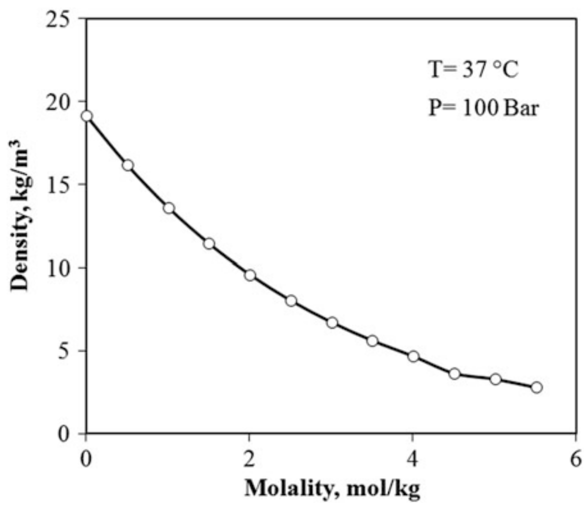


**Fig. 24.6** Density difference (ΔDensity) defined as the difference between the density of fully $CO_2$-saturated brines and brines without dissolved $CO_2$. The difference is getting lower and lower as the salinity increases, mainly because of the salting-out effect leading to decreasing $CO_2$ solubility with increasing salinity. Calculations done by R. Miri using the SAFT-EOS approach

## 24.5 $CO_2$ Trapping Mechanisms

Four mechanisms are commonly considered responsible for keeping $CO_2$ underground after injection: (1) structural trapping; (2) capillary or residual trapping; (3) solubility trapping; and (4) mineral trapping (Benson and Cole 2008). The risk of leakages and the time dependency of risk are related to these four mechanisms (see Fig. 6 in Benson and Cole 2008).

### *24.5.1 Structural Trapping*

At short time-scales (during the injection period), most $CO_2$ will be a separate buoyant phase. The vertical rock permeability and the density contrast between the formation water and $scCO_2$ (see Fig. 24.3) will determine the upward flux of $CO_2$. Chapter 12 and Sect. 1.8 provide an overview of structural elements that can prevent vertical migration of $CO_2$ or hydrocarbons.

### 24.5.2 Capillary (Residual) Trapping

As $CO_2$ flows upwards and laterally below structural or stratigraphic elements, water must be displaced. Such displacement of a wetting fluid by a non-wetting fluid is termed drainage. In siliciclastic reservoirs, mineral grains will be water-wet, and a thin film of water will therefore remain on the mineral grains after a $CO_2$ sweep. If water later flows through the area rich in free $CO_2$, some bubbles of $CO_2$ may not be able to overcome the capillary entry pressure of the smaller pore throats, and will be trapped. The latter process is termed imbibition. In modelling drainage and imbibition, the relation between the water and $CO_2$ saturations and the relative permeabilities must be known. The van Genuchten model is one of several ways of relating relative permeabilities to $CO_2$ and $H_2O$ saturations (van Genuchten 1980). The model is empirical and requires experimental data. Values for irreducible saturations, which are the minimum saturation values $CO_2$ and $H_2O$ can have, and the shape of the saturation/permeability curves, depend on factors such as sediment sorting and mineral grain size.

### 24.5.3 Solubility Trapping

Injected $CO_2$ will first occur primarily as a free phase, but will start to dissolve in the formation water. The rate of dissolution depends on factors such as the $CO_2$/water interface surface area, and diffusion of dissolved $CO_2$ away from the interface. Solubility trapping will therefore be most efficient in heterogeneous reservoirs where the $CO_2$ plume spreads over larger volumes of the reservoir providing more interfacial surface area between $CO_2$ and formation water. The amount of dissolved molecular $CO_2$ depends on factors such as the $CO_2$ partial pressure, temperature and salinity, and can be generally expressed by:

$$x_{CO_2} = \frac{P_{CO_2}\phi}{K_H\gamma}, \tag{24.2}$$

where $x$ is mole fraction, $\phi$ and $\gamma$ are the fugacity and activity coefficients of $CO_2$, and $K_H$ is the Henry's law coefficient. The molecular $CO_2$ reacts with water to form carbonic acid, which dissociates in two steps to form bicarbonate and carbonate:

$$\begin{aligned} CO_2 + H_2O &= H_2CO_3 \\ H_2CO_3 &= HCO_3^- + H^+, \\ HCO_3^- &= CO_3^{2-} + H^+ \end{aligned} \tag{24.3}$$

where the equal sign ('=') denotes equilibrium. Both the Henry's law constant and the equilibrium constants for the carbon speciation are temperature and pressure dependent. As a result of the $CO_2$ dissolution, pH drops to 3 or even lower at the $CO_2$ pressures encountered during $CO_2$ storage.

Because new interfaces between the undissolved $CO_2$ and formation water are constantly made through the mobilisation of the free-phase $CO_2$, or through density-driven mixing of $CO_2$ and formation water, more and more $CO_2$ dissolves with time. Dissolution is therefore favoured in sloping aquifers where the $CO_2$/water interface is large and in heterogenous reservoirs where the plume spreads through a larger volume (Fig. 24.7). If vertical mixing through density-driven plume formation can occur (see last part of Sect. 24.4), then this will promote further dissolution.

### 24.5.4 Mineral Trapping ($CO_2$ Carbonatisation)

The increased acidity of the formation water resulting from $CO_2$ dissolution increases the solubility of the primary minerals (i.e. minerals in the reservoir prior to $CO_2$ injection), leading to dissolution of these phases and precipitation of a new stable mineral assemblage. The rate of dissolution varies from mineral to mineral and is strongly a function of the reservoir temperature. From the primary phases, the clay minerals, feldspars and carbonates play important roles during $CO_2$ storage. Primary carbonates such as calcite dissolve fast (within days) and transform some of the carbonic acid to alkalinity ($HCO_3^-$), buffering some of the pH drop induced by the $CO_2$:

$$CaCO_3 + H_2CO_3 = Ca^{2+} + 2HCO_3^-. \tag{24.4}$$

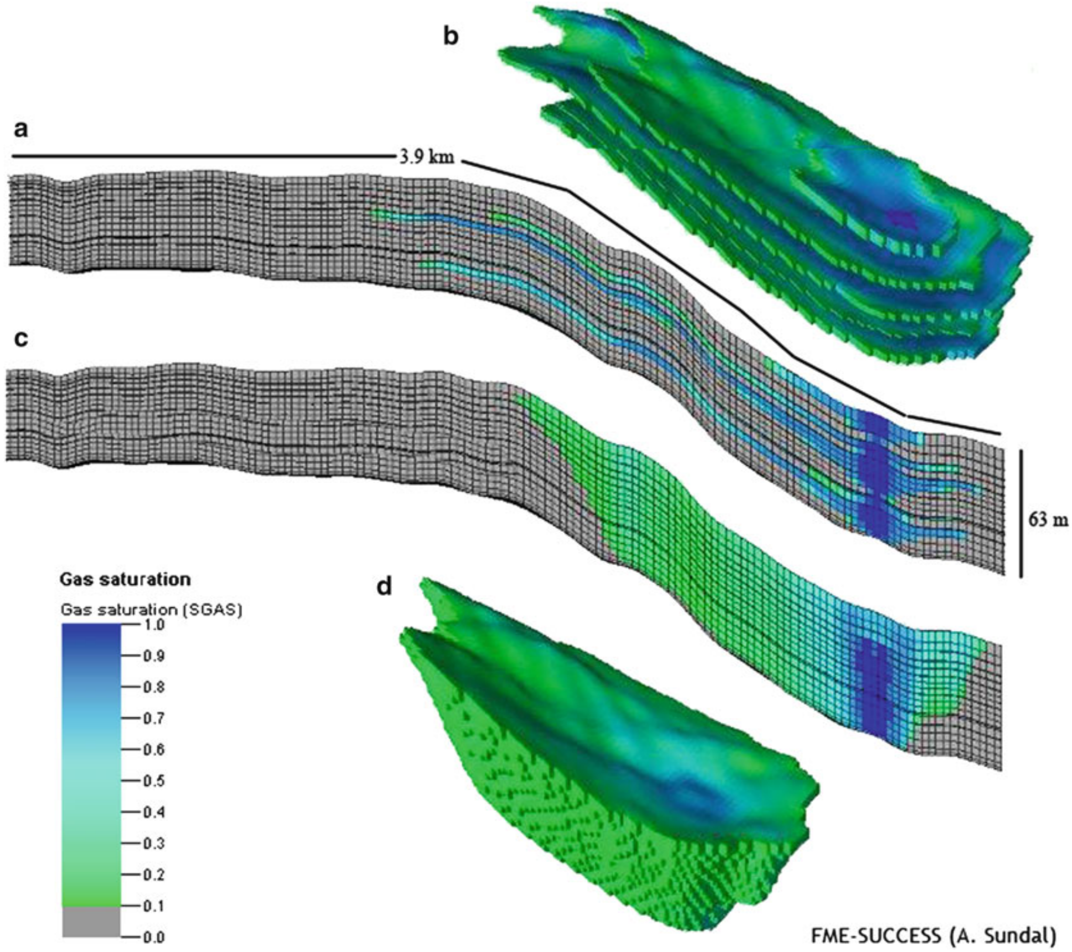


**Fig. 24.7** Injection of $CO_2$ in the Johansen Formation (modified from Sundal et al. 2014). Plume distributions after 20 years. (**a**, **b**) Case #1 includes 15 thin flow baffles. (**c**, **d**) Case #2 Harmonic mean averaged model, Kz = 0.082 mD. Including the flow baffles leads to significantly larger lateral spread of the plume

The pH commonly increases from about 3 to 5 in this reaction (Pham et al. 2011). The rates of feldspar and clay mineral dissolution are many orders of magnitude slower than for carbonate dissolution, especially at low temperatures. These reactions however play important roles in the immobilisation of $CO_2$ in the long term, i.e. mineral trapping of $CO_2$. Clay minerals, such as chlorites, contain divalent metal cations ($Me^{2+}$) that can react with dissolved $CO_2$ and form secondary carbonates (the inverse of reaction 24.4). The most common secondary $Me^{2+}$-carbonates predicted to form during $CO_2$ storage are ankerites ($CaFe_xMg_{1-x}(CO_3)_2$, with $x \leq 1$), siderite ($FeCO_3$), and in some cases disordered dolomite and magnesite. The formation of the latter two in numerical simulations may however be an artifact of the kinetic models being used overpredicting rates of Mg-carbonate formation (Hellevang and Aagaard 2013, Hellevang et al. 2013). Feldspars release $Ca^{2+}$ and $Na^+$, supporting calcite, ankerite and dawsonite ($NaAl(OH)_2CO_3$) formation. In many quartz-rich reservoirs that are poor in $Me^{2+}$, both simulations (e.g. Johnson et al. 2004) and natural observations (e.g. Gao et al. 2009) have suggested that dawsonite may be the dominant secondary carbonate that forms and traps $CO_2$.

Estimates of the mineral-trapping potential of a reservoir require prediction of the following: (1) the amount (volume) of formation water being affected by the $CO_2$ injection, which depends on the drainage pathway; (2) the representative average primary and secondary mineralogy; and (3) the dissolution rates of the primary minerals and growth rates of secondary phases. All these points require a good understanding of the depositional environment and the diagenetic

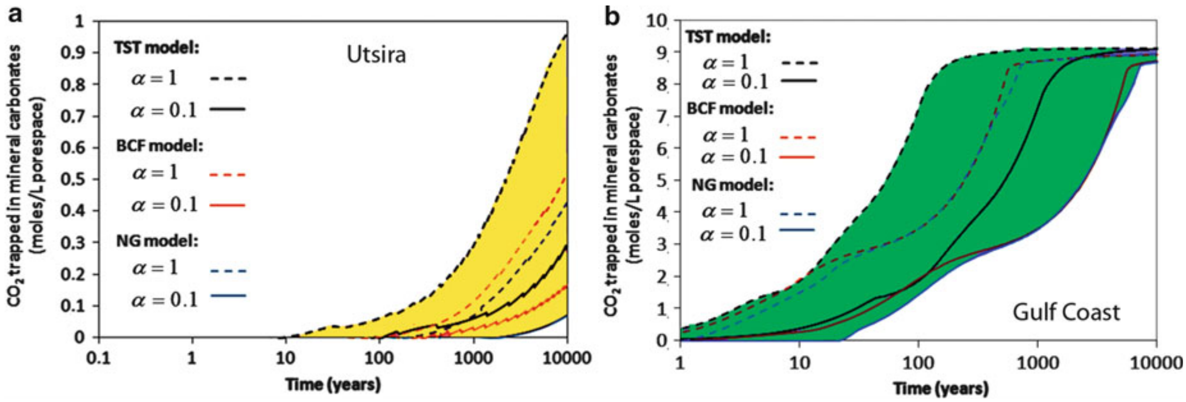


**Fig. 24.8** $CO_2$ carbonatisation potential for (**a**) Utsira Sand; and (**b**) Gulf Coast sediments (modified from Hellevang and Aagaard 2013). The figure shows that the total amount of carbonates that can form (~10 times more in Gulf Coast sediments) depends strongly on the initial sediment composition, and that the range in predictions using different kinetic models is very large. 'Alpha' here denotes fraction of the mineral surface area being reactive (see Hellevang et al. 2013)

overprint. In the kinetic models, reactive surface areas are commonly regarded as a highly uncertain parameter. Knowledge on how much of the surfaces of reactive minerals (e.g. feldspars and chlorites) are in contact with the formation water (provides the specific surface area as $m^2$/L porewater) is therefore essential. Figure 24.8 shows predictions of the long-term trapping potential for two reservoirs, the Utsira Sand, and a representative of a feldspar-rich Gulf Coast sediment (Frio Formation, Lower Tertiary). The figure shows how reducing the reactive surface area by one order of magnitude (parameter $\alpha$) has a large impact on the predictions, and that the three different kinetic models used also lead to a large range in predicted carbonatisation. Because of the uncertainties in the kinetic models, there is at present a focus to improve both the kinetic models and the parameters used in the models.

## 24.6 How Can We Know that $CO_2$ Is Safely Stored?

To ensure that the $CO_2$ is safely stored underground, various monitoring technologies are in use, with seismic and well-pressure monitoring being two important methods. Seismic monitoring is built on comparing seismic signals in time and space, so called time-lapse or 4D seismics (see Chap. 19). By doing so, the difference in the density of supercritical $CO_2$ (approximately 400–800 kg/$m^3$) and water (approximately 1,030–1,100 kg/$m^3$) is used to map the extent of the $CO_2$ plume. This method has been very successful in monitoring the $CO_2$ plume migration for the Sleipner injection (Eiken et al. 2011). Microseismicity caused by fracture or fault activation may also provide valuable information on the effect of pressure build-up and fluid migration in the sub-surface. The status of $CO_2$ storage operations is obtained indirectly by monitoring the reservoir pressure. If the pressure approaches the estimated cap-rock fracture pressure, preventative measures have to be taken. Such measures can be reduction of the injection rate or water production. However, in some cases, such as for the Tubåen Formation at Snøhvit, the storage capacity is very limited and alternative storage reservoirs have to be found. In most cases, a combination of seismic monitoring and measurements of the well pressures is employed.

## 24.7 Examples of $CO_2$ Storage Projects

There are today (October 2013) 12 CCS projects that are operational, but a large number of others are in the planning and executive phases (Global CCS Institute). One of the projects that has received most attention is at Sleipner (North Sea), being the first industrial-scale dedicated CCS project started in 1996. Some projects such as In Salah, Algeria, were running until recently, but that project ended after illustrating how several monitoring technologies can be used to successfully track the fate of stored $CO_2$. Below is a short overview of the Sleipner, Snøhvit (Barents Sea), In Salah, and Weyburn-Midale (Saskatchewan, Canada) CCS projects.

### 24.7.1 Sleipner CCS Project

Natural gas produced at Sleipner contains about 9.5% $CO_2$. In order to ship this natural gas in a liquid form (LNG) to customers it has to be cooled to −162°C, which may cause formation of $CO_2$ ice aggregates. To avoid this, most of the $CO_2$ is captured during production, i.e. removed from the natural gas stream. Before 1996, $CO_2$ captured from the Sleipner field was released directly to the atmosphere. A few years before, in 1991, Norway had established a tax on $CO_2$ emissions (in 1999, about 18 US$/ton $CO_2$ on emissions of ~1 Mt $CO_2$/year). This represented a considerable financial levy on the operators of Sleipner. In 1996, Statoil and partners started to inject $CO_2$ captured at Sleipner into the Utsira Formation, and the injection has continued successfully at a rate of approximately 1 Mt $CO_2$/year.

The CCS operation at Sleipner was feasible because of the properties of the Utsira storage reservoir located near the Sleipner field. The Utsira Sand sediments are basin-restricted marine lowstand deposits of Miocene-Pliocene age (Zweigel et al. 2004), only weakly compacted and with high porosity (30–40%). The sand is very extensive (see Fig. 24.1) and is in many ways an optimal storage reservoir. At 800 m below seafloor, temperatures and pressures are about 37°C and 100 bar, which is above the critical point of $CO_2$. As overburden, the Utsira Formation has a 250 m clay-rich sequence of the Nordland group which provides the seal, with a further several hundred metres of coarser-grained Quaternary sediments above (Zweigel et al. 2004). The mudstones deform in a ductile manner and stress changes are therefore not expected to lead to fractures that could provide leakage pathways for the $CO_2$.

The injected $CO_2$ has been monitored by 3D seismics surveys carried out before, and several times after, injection started in 1996. The seismic images show that $CO_2$ has spread out laterally below nine distinct stratigraphic layers. A bulk of the $CO_2$ is still trapped under these layers and this has reduced the amount of free $CO_2$ that has reached the cap rock (Hermanrud et al. 2009). A much discussed feature of the seismic images is the presence of a chimney-like structure in the storage reservoir just above the injector. This structure possibly formed shortly after injection commenced, by liquefaction of the sediments breaking up the thin intra-reservoir shale layers (Hermanrud et al. 2009). Although $CO_2$ has migrated through what was thought to be a tight shale layer in the cap-rock and into an overlaying sand wedge, there are no indications of further leakage to shallower depths.

### 24.7.2 Snøhvit CCS Project

Gas produced from the Lower to Middle Jurassic Stø Formation at Snøhvit contains 5–8% $CO_2$. This gas is transported by pipelines to the processing plant at Melkøya, where $CO_2$ is captured and transported back underground. $CO_2$ storage started in 2008 with injection into the early Jurassic Tubåen Formation, which lies just below the gas-producing Stø Formation In contrast to the Utsira Sand, the stratigraphic sequences in the Barents Sea region have experienced a complex history of burial and later tectonic uplift. The present-day depth of the Tubåen is about 2,400 m at the injection site, and temperature and pressure before injection were 95°C (Hansen et al. 2013) and 240 bars (assuming hydrostatic). The depth and temperature at maximum burial may however have been more than 3,200 m and 130°C. After a short period of injection, the operation experienced problems with rapid pressure build-up, interpreted to be caused by reactions clogging the pore space and reducing the permeability around the well (Hansen et al. 2013). In the Tubåen Formation, these reactions could be: (1) salt formation (scale) caused by the drying-out of highly saline brine around the well; or (2) $CO_2$ hydrate (clathrate) formation. As $CO_2$ entered the reservoir at low temperature (4°C) and pressures were higher than 290 bars (Hansen et al. 2013), the latter is more likely (Kvamme and Tanaka 1995, Duan and Sun 2006), although the highly saline brine depresses the freezing point of $CO_2$ hydrate (Duan and Sun 2006). Salt (halite) formation caused by injection of dry $CO_2$ has been predicted numerically (Muller et al. 2009) and in laboratory experiments (Bacci et al. 2013), and although not yet observed *in situ*, could also very well be the reason for the pressure build-up. After the initial pressure build-up was solved by chemical treatment, the operation continued. Unfortunately, the tight and compartmentalised Tubåen Formation turned out to have only a limited storage capacity, and pressure continued to increase until injection was abandoned in 2011. Injection was then moved to the shallower Stø Formation, below the gas reserves. As $CO_2$ migrates updip and will mix with the natural gas, there is an expectance that additional storage sites will be needed in the future to continue the $CO_2$ storage operation.

### 24.7.3 In Salah CCS Project

The In Salah CCS project in central Algeria is an example of an onshore CCS operation. During the lifetime of the project, between 2004 and 2011, 3.8 Mt $CO_2$ was stored in a Carboniferous sandstone unit 1.9 km below the surface. The project demonstrated a large number of monitoring technologies, such as the use of Interferometric Synthetic Aperture Radar (InSar) to monitor surface heave, 4D seismics to track the underground $CO_2$ migration, geophones to detect microseismicity, well-head sampling of geochemical tracers, etc. (Ringrose et al. 2013 and references therein). The combination of all these technologies enabled the tracking both of possible hydrofractures and potential migration of the $CO_2$ outside the Krechba hydrocarbon lease, and remedial action (operation and monitoring responses). The In Salah CCS project has therefore provided highly valuable information on the whole chain, from planning to operation and abandonment.

### 24.7.4 Weyburn-Midale CCS-EOR Project

The Weyburn-Midale project is at present the world's largest CCS operation, and is an example of a CCS Enhanced Oil Recovery (EOR) project. The CCS operation started in 2000, and currently nearly 3 Mt $CO_2$ are annually injected in multiple wells and used for enhanced oil recovery (Whittaker et al. 2011). At the planned end of the operation, in 2035, the amount of stored $CO_2$ is expected to be more than 40 Mt. The injected $CO_2$ is a byproduct of coal gasification at the Great Plains Synfuels Plant in North Dakota, USA.

The target reservoirs are of lower Carboniferous age, at a present-day depth of 1,300–1,500 m. The rocks were deposited in a peritidal sequence, with carbonates deposited at highstands and evaporitic dolomites formed at lowstands. The total storage capacity of the Weyburn-Midale reservoirs, including both the EOR phase and later $CO_2$ storage, is estimated to be between 50 and 60 Mt. The Weyburn-Midale $CO_2$ monitoring and storage project, supported by the International Energy Agency Greenhouse Gas R&D program (IEA GHG), has invested in an extensive geophysical and geochemical monitoring programme, including passive seismic and soil gas and fluid geochemistry monitoring (Whittaker et al. 2011).

## 24.8 What Is the Future of CCS?

The main obstacles to implementing CCS on a large scale today are high costs and, for many regions, a lack of a market for $CO_2$. In North America, $CO_2$ has been used for enhanced oil recovery for decades, and this illustrates that the costs of capture and transport can be more than compensated if a market exists to sell the $CO_2$. A second challenge is that the cost of releasing $CO_2$ to the atmosphere is still too low to make it financially viable for most emitters to store $CO_2$. Below is a short review of present-day activities to utilise and store $CO_2$ in the USA, and a suggested solution to lower the cost and allow large-scale storage by gathering emissions from many point sources into one shared pipeline network and storage site.

### 24.8.1 CCUS/EOR

CCUS (and CCUS/EOR), is short for Carbon Capture Use (or Utilization) and Storage, and Enhanced Oil Recovery (EOR). By using captured $CO_2$ in industrial processes such as EOR, CCS may become profitable. There are at present nine CCUS/EOR projects in the operational phase and several in the planning and executive stage, most of them in the USA (Global CCS Institute, Oct. 2013). Of these, the largest-scale is the Weyburn-Midale CCS-EOR project described above.

Onshore CCUS/EOR has been a great success. The same is not yet true for offshore CCUS/EOR. There are several reasons for this: (1) seawater is readily available offshore and can be used instead of the less available $CO_2$; (2) the costs of installing $CO_2$ capture facilities may be considerable; (3) injected $CO_2$ can lead to corrosion of already existing infrastructure (wells etc.) and investment in new infrastructure (in addition to the capture facilities) may be required; (4) stored $CO_2$ may be produced back along with the oil. Whether CCS/EOR will be implemented offshore on a larger scale in the future depends on the cost-benefit picture and the availability of $CO_2$. There are limits to the degree that water can enhance oil recovery, and $CO_2$ is known to further increase the amount of oil that can be extracted and thus extend the lifetime of oil fields. Moreover, new technologies using $CO_2$ for EOR are being developed. One recent discovery is that $CO_2$ foams (rather than gas or supercritical) can significantly improve the recovery of medium to heavy oils and that foams are twice as effective compared to water or gas/supercritical $CO_2$ (Rassenfoss 2012).

### 24.8.2 Large Scale Transport and Storage

Most of the discussion so far has been on capture and storage from single point sources. This limits CCS projects to a few Mt/a. The total emissions from point sources in larger regions in Europe, Asia, and America may however reach hundreds of Mt/a. By connecting smaller (<20–40 Mt) $CO_2$ suppliers through hubs, and transporting large amounts (hundreds of Mt/a) to reservoirs such as the Utsira Sand with very large storage capacity, the cost of stored $CO_2$ per ton may be reduced significantly. The cost of pipelines and infrastructure is shared among several stakeholders, and larger dimensions of pipelines allow a greater volume $CO_2$ to be transported per ton steel used (volume/cross-section ratio of pipelines increases). The amount of pressure a pipeline can hold is a function of the diameter of the pipeline, with smaller pipes withstanding higher pressures. The upper limit of pipeline dimensions must therefore be weighed against the pressures required to transport the $CO_2$ as a dense phase.

To allow such large-scale CCS in Europe requires regulations across national boundaries, and there are several complicated issues that must be sorted out. One is the ownership and risk responsibility of the transport and storage of a mixture of $CO_2$ from several sources. Who will be held responsible in case of a pipeline rupture? Who owns the stored $CO_2$ and will be responsible for a monitoring programme? It is natural that in Europe the European Union and associated nations such as Norway, should facilitate such large scale CCS.

## 24.9 Summary

Carbon capture and storage is one out of several strategies to mitigate rapidly increasing atmospheric $CO_2$ levels. CCS involves capture of $CO_2$ from natural gas or flue gas, and transport and storage in geological formations. There are several technologies available for capture, and the choice of technology depends on the processing plant and the cost of operation. Because of the relatively high costs of capture, there are large research programmes underway to improve the energy-efficincy of current methods and to come up with new and more cost-effective capture technologies. The captured $CO_2$ can be stored underground in geological formations, preferentially as a dense supercritical phase, but this also requires large amounts of energy. The main requirements of a storage formation are that it has sufficient injectivity and storage capacity and a tight cap rock. Moreover, as water is mobilised by the injected $CO_2$ and the pressure waves caused by the injection, one has to ensure that freshwater resources are not affected by the storage operation. In the future, to meet the IPCC target of globally storing Gt of $CO_2$ per year rather than the few Mt/a stored today, storage operations will have to be scaled up. One way to do this is to collect $CO_2$ from several large point sources and store it in sandstones, such as the Utsira Sand, that possess a very high storage capacity (Fig. 24.1).

## References


Alemu, B.L., Aagaard, P., Muntz, I.A. and Skurtveit, E. 2011. Caprock interaction with $CO_2$: A laboratory study of reactivity of shale with supercritical $CO_2$ and brine. Applied Geochemistry 26(12), 1975–1989.

Bacci, G., Durucan, S. and Korre, A. 2013. Experimental and numerical study of the effects of halite scaling on injectivity and seal performance during $CO_2$ injection in saline aquifers. Energy Procedia 37, 3275–3282.

Benson, S.M. and Cole, D.R. 2008. $CO_2$ sequestration in deep sedimentary formations. Elements 4, 325–331.

Bjørlykke, K., Mo, A. and Palm, E. 1988. Modelling of thermal convection in sedimentary basins and its relevance to diagenetic reactions. Marine and Petroleum Geology 5, 338–351.

Duan, Z. and Sun, R. 2006. A model to predict phase equilibrium of $CH_4$ and $CO_2$ clathrate hydrate in aqueous electrolyte solutions. American Mineralogist 91, 1346–1354.

Eiken, O., Ringrose, P., Hermanrud, C., Nazarian, B., Torp, T. A. and Høier, L. 2011. Lessons learned from 14 years of CCS operations: Sleipner, In Salah and Snøhvit. Energy Procedia 4, 5541–5548.

Elenius, M.T. and Gasda, S.E. 2013. Convective mixing in formations with horizontal barriers. Advances in Water Resources 62, 499–510.

Figueroa, J.D., Fout, T., Plasynski, S., McIlvried, H. and Srivastava, R.D. 2008. Advances in $CO_2$ capture technology—The U.S. Department of Energy's carbon sequestration program. International Journal of Greenhouse Gas Control 2, 9–20.

Gao, Y., Liu, L. and Hu, W. 2009. Petrology and isotopic geochemistry of dawsonite-bearing sandstones in Hailaer basin, northeastern China. Applied Geochemistry 24, 1724–1738.

Gaus, I., Azaroual, M. and Czernichowski-Lauriol, I. 2005. Reactive transport modelling of the impact of $CO_2$ injection on the clayey cap rock at Sleipner (North Sea). Chemical Geology 217, 319–337.

Global CCS Institute. http://www.globalccsinstitute.com.

Hansen, O., Gilding, D., Nazarian, B., Osdal, B., Ringrose, P., Kristoffersen, J.-B., et al. 2013. Snøhvit: The history of injection and storing 1 Mt $CO_2$ in the fluvial Tubåen Fm. Energy Procedia 37, 3565–3573.

Hellevang, H. and Aagaard, P. 2013. Can the long-term potential for carbonatization and safe long-term $CO_2$ storage in sedimentary formations be predicted? Applied Geochemistry 39, 108–118.

Hellevang, H., Pham, V.H. and Aagaard, P. 2013. Kinetic modeling of $CO_2$-water-rock interactions. International Journal of Greenhouse Gas Control 15, 3–15.

Hermanrud, C., Andresen, T., Eiken, O., Hansen, H., Janbu, A., Lippard, J., et al. 2009. Storage of $CO_2$ in saline aquifers—lessons learned from 10 years of injection into the Utsira Formation in the Sleipner area. Energy Procedia 1, 1997–2004.

IPCC. 2013. Climate change 2013: The physical science basis. In: Stocker, T.F., Quin, D., Plattner, G.-K., Tignor, M., Allen, S.K., Boschung, J., Nauels, A., Xia, Y., Bex, V. and Midgley, P.M. (eds.), Contribution of Working Group I to the Fifth Assessment Report of the Intergovernmental Panel on Climate Change. Cambridge: Cambridge University Press, 1535 pp.

Johnson, J.W., Nitao, J.J. and Knauss, K.G. 2004. Reactive transport modeling of $CO_2$ storage in saline aquifers to elucidate fundamental processes, trapping mechanisms and sequestration partitioning. In: Bains, S.J. and Worden, R.H. (eds.), Geological Storage of Carbon Dioxide. Geological Society Special Publication 233, pp. 107–128.

Kvamme, B. and Tanaka, H. 1995. Thermodynamic stability of hydrates for ethane, ethylene, and carbon dioxide. Journal of Physical Chemistry 99, 7114–7119.

Lu, J., Wilkinson, M., Haszeldine, R.S. and Fallick, A.E. 2009. Long-term performance of a mudrock seal in natural $CO_2$ storage. Geology 37, 35–38.

Muller, N., Qi, R., Mackie, E., Pruess, K. and Blunt, M.J. 2009. $CO_2$ injection impairment due to halite precipitation. Energy Procedia 1, 3507–3514.

Pham, T.H.V., Maast, T.E., Hellevang, H. and Aagaard, P. 2011. Numerical modeling including hysteresis properties for $CO_2$ storage in Tubåen Formation, Snøhvit field, Barents Sea. Energy Procedia 4, 3746–3753.

Rassenfoss, S. 2012. Increased oil production with something old, something new. Journal of Petroleum Technology, Oct. issue, 36–39.

Ringrose, P.S., Mathieson, A.S., Wright, I.W., Selama, F., Hansen, O., Bissell, R., et al. 2013. The In Salah $CO_2$ storage project: lessons learned and knowledge transfer. Energy Procedia 37, 6226–6236.

Sundal, A., Hellevang, H., Miri, R. and Aagaard, P. 2014. On layer specific $CO_2$ plume distributions and variability in mineralization potential. Submitted to the Fourth EAGE $CO_2$ Geological Storage Workshop, Stavanger, April 23–25, 2014.

van Genuchten, M.Th. 1980. A closed-form equation for predicting the hydraulic conductivity of unsaturated soils. Soil Science Society of America Journal 44, 892–898.

Whittaker, S., Rostron, B., Hawkes, C., Gardner, C., White, D., Johnson, J., et al. 2011. A decade of $CO_2$ injection into depleting oil fields: monitoring and research activities of the IEA GHG Weyburn-Midale $CO_2$ monitoring and storage project. Energy Procedia 4, 6069–6076.

Zabaloy, M.S., Vasquez, V.R. and Macedo, E.A. 2005. Viscosity of pure supercritical fluids. Journal of Supercritical Fluids 36, 106–117.

Zweigel, P., Arts, R., Lothe, A.E. and Lindeberg, E.G. 2004. Reservoir geology of the Utsira Formation at the first industrial-scale underground $CO_2$ storage site (Sleipner area, North Sea). In: Baines, S.J. and Worden, R.H. (eds.), Geological Storage of Carbon Dioxide. Geological Society Special Publication 233, pp. 165–180.